REFINING REGIONAL GRAVITY FIELD SOLUTIONS WITH GOCE GRAVITY GRADIENTS FOR CRYOSPHERIC INVESTIGATIONS

Daniel Rieser[(1)], Roland Pail[(2)], Aleksey I. Sharov[(3)]

[(1)]Institute of Navigation and Satellite Geodesy, Graz University of Technology, Steyrergasse 30/II, 8010 Graz, Austria, Email:daniel.rieser@tugraz.at
[(2)]Institute for Astronomical and Physical Geodesy, Technische Universität Muenchen, Arcisstr. 21, 80333 Muenchen, Germany, Email:pail@bv.tum.de
[(3)]Institute of Digital Image Processing, Joanneum Research, Wastiangasse 6, 8010 Graz, Austria, Email: sharov@joanneum.at

ABSTRACT

In this paper, the ability of GOCE gravity gradient observations for refining regional geoid solutions is investigated for a restricted area of interest using Least Squares Collocation (LSC). GOCE data from November 2009, reflecting the medium wavelength signal part of the gravity field, are combined with terrestrial gravity anomalies simulated from EGM2008. The gravity gradients are available in the Gradiometer Reference Frame (GRF), hence a computation method independent of the reference frame is implemented. Due to the presence of coloured noise, GOCE gradients are filtered with an adapted Wiener filter. Two different solution strategies for a regional geoid solution are developed and implemented. In the following results using real GOCE data, terrestrial data and their combination are presented and compared. It is shown that GOCE improves the geoid solution in the medium wavelength of the gravity signal spectrum considerably.

1. INTRODUCTION

With the launch of the GOCE gravity field mission in March 2009 new types of observations in terms of gravity gradients at satellite altitude are available. These measurements are covering the whole globe in large number and are primarily used for the determination of high precision global gravity field models [8]. However, the unique observations of the second derivative of the gravitational potential have a very dense data distribution especially in high latitudes due to the GOCE orbit configuration, c.f. Fig. 1. Therefore the use of gradients as in situ measurements can also provide valuable information for the determination of regional gravity fields that form a basis for investigations e.g. on the interaction of snow-ice cover variations and the gravity field as performed within the ICEAGE research project [7]. As main study area a region in the Barents-Kara sector covering the area of the largest European ice cap on the North of the Novaya Zemlya island is defined.

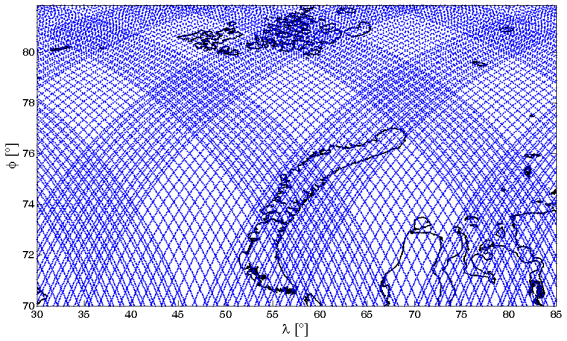

Figure 1. GOCE ground tracks over the Eurasian Arctic for November2009

At a regional scale like this Least Squares Collocation (LSC) [5] is a standard method for the computation of the Earth's gravity field. Its tremendous advantage is the ability to combine various kinds of gravity field signals, e.g. geoid undulations, gravity anomalies or gravity gradients as measured by GOCE. Hence, with LSC it is possible to cover a broad range of the gravity field's signal spectrum by the combination of terrestrial gravity anomalies data representing the high frequency gravity field signal part, a global gravity model (e.g. from GRACE) accounting for the low frequency gravity field signals. The GOCE mission is expected to provide accurate gravity information especially in the medium wavelength spectrum, which is superior to the other two data types.

Using GOCE gradients in LSC requires the derivation of suitable covariance expressions for second and lower order derivatives of the anomalous gravity potential. A scientific problem arises due to the fact that the GOCE mission observes gradients in the satellite sensor frame, the Gradiometer Reference Frame (GRF). This is deviating from an ideal Local Orbit Reference Frame (LORF), in which the X-axis is defined by the actual flight direction, the Z-axis is pointing towards the Earth's center and the third axis is completing an orthogonal Cartesian coordinate frame, by several degrees [6]. However, gravity field quantities are

Proc. 'ESA Living Planet Symposium', Bergen, Norway 28 June – 2 July 2010 (ESA SP-686, December 2010)

derived with LSC in a Local North Oriented Frame (LNOF) defining a local geographical coordinate frame. In the case of the GOCE gradiometer, the key problem is that not all the gravity gradient components can be measured with the same level of accuracy, which is due to the specific orientation of the individual accelerometers composing the gradiometer assembly. In fact, the accuracy of the off-diagonal elements V_{XY} and V_{YZ} is degraded by a factor of 100 to 1000 [2]. Therefore a rotation of the gradient tensor from GRF to LORF or GRF to LNOF must be avoided since otherwise the large errors of the off-diagonal elements would be propagated to all other components and drastically deteriorate the well-measured gradients [6]. Alternatively, the base functions (i.e. the covariance matrices) of LSC given in LNOF have to be rotated to the GRF.

Additionally, it has to be considered that GOCE's gravity gradiometer instrument only shows good performance in the measurement bandwidth between 5 and 100 mHz. The gradient data comprise measurement errors in terms of coloured noise in particular in the long-wavelength fraction of the gravity signal. To reduce these effects an a-priori filtering step has to be introduced. Here the standard Wiener filter method for filtering GOCE gravity gradients [3, 9] is adapted for the data set within the investigated region. This method is similar to the one implemented in the space-wise approach for the computation of global gravity field models for GOCE data [4].

In order to cope with the above mentioned issues, theoretical concepts are summarized and adapted for a suitable treatment of real GOCE gradients in the frame of the LSC process.

2. THEORETICAL AND METHODOLOGICAL CONCEPTS

2.1. Least Squares Collocation (LSC)

According to the theory of LSC, [5], any arbitrary gravity field signal s can be predicted, if the linear functional which relates the signal to the basic disturbing potential T is applied to the covariance model of T in terms of a covariance propagation. The basic formula of LSC is given by

$$s = C_{sl}(C_{ll} + C_{nn})^{-1} l \tag{1}$$

where C_{sl} consists of the cross-covariances between the signal s and the observation l, while C_{ll} is the auto-covariance matrix of the observations themselves, whose error structure is introduced by the noise-covariance matrix C_{nn}. The entries of C_{sl} and C_{ll} can be calculated from a covariance function of the anomalous potential which, can be expressed as

$$C(r_i, r_j, \psi_{ij}) = \sum_{n=N_{\min}}^{N_{\max}} k_n \left(\frac{R^2}{r_i r_j} \right) P_n(\cos\psi_{ij}) \tag{2}$$

It depends on the radius R of a sphere completely enclosed by the Earth, the distance r_i, r_j from the geocenter to the observation stations, and the Legendre polynomials P_n of degree n, which are functions of the cosine of the spherical distance ψ_{ij} between the stations. The signal variances k_n can bee obtained from the fully normalized harmonic coefficients of an gravity field model via the relation

$$k_n = \sum_{m=0}^{n} \left[\overline{C}_{nm}^2 + \overline{S}_{nm}^2 \right] \tag{3}$$

While the functional that relates the vertical gravity gradient T_{ZZ} to the anomalous potential T is simply given by the second order radial derivative, the functionals for all other gradients are more complex. For instance, the T_{XX} gradient can be expressed in terms of spherical coordinates by

$$T_{XX} = \left(\frac{1}{r}\frac{\partial}{\partial r} + \frac{1}{r^2}\frac{\partial^2}{\partial^2 \varphi} \right) T \tag{4}$$

To derive the covariance between gradients T_{XX} at different positions, the functional of Eq. 4 has to be applied twice to the covariance function in Eq. 2, once for each position, leading to

$$\begin{aligned} &\operatorname{cov}(T_{XX}, T_{X'X'}) = \\ &\frac{1}{r}\frac{\partial}{\partial r} + \frac{1}{r^2}\frac{\partial^2}{\partial \varphi^2}\left(\frac{1}{r'}\frac{\partial C}{\partial r'} + \frac{1}{r'^2}\frac{\partial^2 C}{\partial \varphi'^2} \right) \end{aligned} \tag{5}$$

It can be seen, that the covariance propagation for gravity gradients leads to partial derivatives of the basic covariance model C up to a maximum order of four. In order to calculate all necessary covariances of derivatives of T, an approach as in [13] can provide a convenient solution to the problem. Here the covariances are computed as a combination of base functions t_{ij} ($t = \cos\psi$) and K_{ij}, where

$$t_{i0} = r\frac{\partial t}{\partial x_i}, \; t_{0j} = r'\frac{\partial t}{\partial y_j}, \; t_{ij} = rr'\frac{\partial^2 t}{\partial x_i \partial y_j} \tag{6}$$

with x_i, $i = 1...3$ and y_j, $j = 1...3$ representing the local Cartesian coordinates at two different points. The second kind of base functions are derivatives of the covariance model with respect to the stations radii r_i, r_j, and/or with respect to t

$$K_{ij}^{k} = r^{n} r'^{m} \frac{\partial^{i}}{\partial t^{i}} \frac{\partial^{j} C(r,r',t)}{\partial r^{n} \partial r'^{m}}$$
$$\cdots \begin{cases} n+m=j \\ i+j \le 4 \end{cases}, \quad k = \begin{cases} 1 \ldots n=m=1 \\ 0 \end{cases} \tag{7}$$

Since the covariance model is in principle a series of Legendre polynomials, a recursion algorithm to calculate this sum as well as their derivatives is applied as in [11] and [12]. The covariances of all derivatives of T up to the second order between two stations can then be expressed by a 4 x 4 matrix

$$C_{ijmn} = \mathrm{cov}\left(\frac{\partial^2 T}{\partial x_i \partial x_j}, \frac{\partial^2 T}{\partial y_m \partial y_n} \right) \tag{8}$$

where the subscripts i, j and m, n, resp., stand for the derivatives with respect to the local coordinates of the evaluation stations. An advantage of this approach is the possibility to perform covariance propagation to another reference frame quite easily. It can be achieved by rotation of the permutations of the covariance matrix of a specific derivative at one station Q

$$C_{ij}^{rot} = R_Q C_{ij}(m,n) R_Q{}^{T}, \quad m=n=1 \ldots 3 \tag{9}$$

and a consecutive rotation of the permutations at the other station P

$$C_{mn}^{rot} = R_P C_{mn}(i,j) R_P{}^{T}, \quad i=j=1 \ldots 3 \tag{10}$$

2.2. Filtering gradient data

As mentioned in the introduction, the 6 accelerometers integrated in the GOCE gradiometer show a good performance only in the measurement bandwidth of 5 to 100 mHz, while the performance below and above this measurement bandwidth is significantly worse (c.f. Fig. 2).

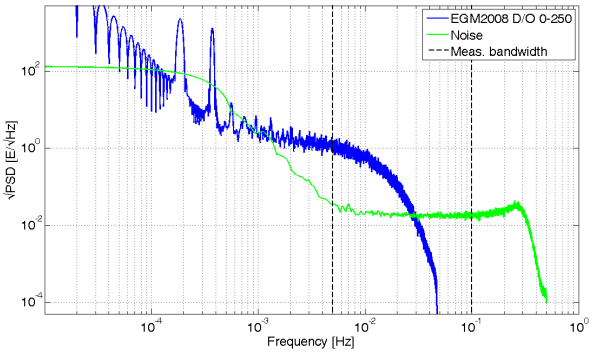

Figure 2. PSD of GOCE V_{ZZ} gradients simulated from EGM2008 (up to degree/order 250) in blue and the corresponding noise PSD in green

Especially the large long-wavelength errors lead to highly correlated observations along the short orbit tracks crossing the test area. In order to reduce the noise a filtering step is introduced, following the Wiener filter theory [9, 1]. Such a filter is also applied within the 'space-wise approach' concept of GOCE HPF WP 7000 [3, 4].
This method assumes that a gravity gradient time series t consists of signal component s and a noise component n

$$t = s + n \tag{11}$$

The Wiener filter W in the spectral domain can then be defined as

$$W = \frac{S_s}{S_s + S_n} \tag{12}$$

where S_s and S_n are the power spectral densities (PSD) of signal s and noise n, respectively, and can be derived by squaring the according Fourier transforms. The filtered signal $\hat{s}$ in the time domain follows from

$$\hat{s} = F^{-1}\left[W \cdot F_t \right] \tag{13}$$

which is the inverse Fourier transform of the product of the Wiener filter W and the Fourier transform F_t of the time series.

The filter error e of the estimate $\hat{s}$ with respect to the (in fact unknown) true signal s, is given by

$$e = \hat{s} - s \tag{14}$$

Hence a corresponding error covariance function can be derived according to

$$C_{ee} = F^{-1}\left[\frac{S_s \cdot S_n}{S_s + S_n} \right] \tag{15}$$

This is true since the Fourier transform of a signal's autocovariance function, e.g. C_{ee}, equals the PSD of the signal itself. With this step a consistent stochastic modelling of the error structure of the filtered signal is achieved, which is of great importance for a successful performance of the LSC processing, c.f. Eq. 1.

2.3. Methodological restrictions and solution strategies

As addressed in the introduction, the low-accuracy gradient tensor components V_{XY} and V_{YZ} make it

impossible to rotate the gradient observations measured in GRF to another reference frame without having a negative impact on the accuracy of the well-determined gradient types. For LSC this means that the corresponding covariances have to be rotated to the GRF instead, which can be performed as outlined in section 2.1. Though, there is a theoretical restriction imprinted by the Wiener filtering processing step. The observed gravitational gradients in the GRF can not be considered as a signal stationary in time. However, in case of the Wiener filter theory, stationarity is a basic precondition, which is fulfilled in LORF, as explained in [1].

As a consequence, different solution strategies can be considered. The first one is to neglect this theoretical requirement and to set the GRF as computational reference frame (c.f. Fig. 3). This implies that the covariance matrix entries of C_{sl} and C_{ll} related to gradient observations in the LSC concept (c.f. Eq. 1) have to be rotated to the GRF. Further, Wiener filtering is directly applied to the gradient time series in GRF. Assuming that the gradient components are uncorrelated amongst each other, the error covariance function of the filtered signal (Eq. 15) can be used to set up the corresponding noise-covariance matrix C_{nn} for LSC in GRF.

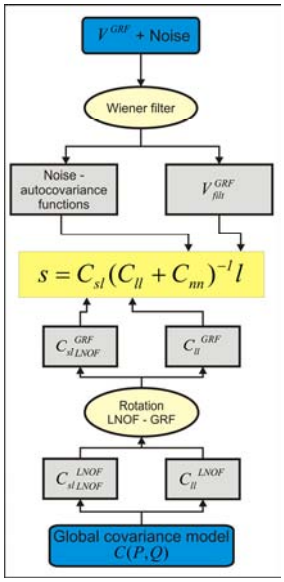

Figure 3. Solution strategy 1.

The second approach (c.f. Fig. 4) is to replace the critical gradients V_{XY} and V_{YZ} with external information, i.e. the two components are derived from a gravity model in GRF. Such a gravity model can be e.g. EGM2008, or in future, a GOCE gravity model, which would be favourable since gradients computed from this model would be most consistent to the original observations. After this replacement the gradients can be rotated from GRF to LORF, where the Wiener filtering can be applied in strict sense. As now the LORF serves as computational frame, covariances of gradients have to be rotated to LORF as well in the already described manner. However, also this strategy bears some problems, because the rotation of gradients from GRF to LORF requires a consistent covariance propagation of the noise-covariance matrix C_{nn}. Hence, C_{nn} has to be set up in the GRF using a-priori information of the error structure of the observations.

For the replaced components V_{XY} and V_{YZ}, a covariance propagation of the gravity model can be performed. To get error information of the real gradient observations in GRF, preceding Wiener filtering step is performed for each gradient type, accepting that this is only an approximation. With the resulting covariance functions given in Eq. 15, C_{nn} can then be set up in GRF and afterwards rotated into LORF. As a consequence, the noise-covariances of the gradients are now correlated and a consistent stochastic modelling of the error structure is obtained.

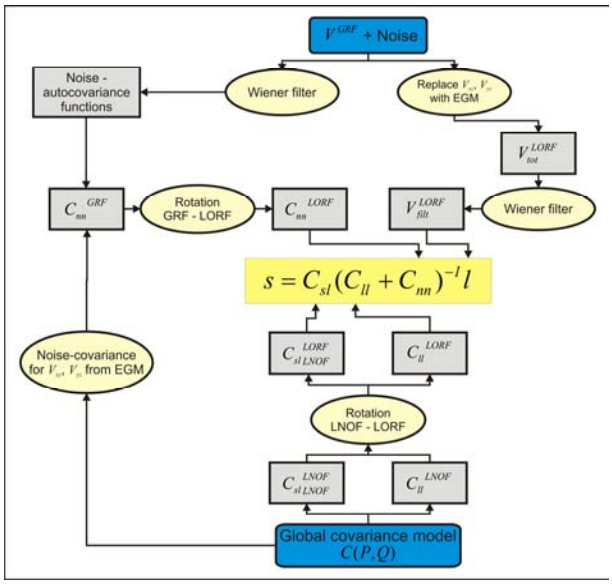

Figure 4. Solution strategy 2

3. GEOID COMPUTATION WITH GOCE GRADIENTS

In this study the GOCE Level-1b data set for November 2009 available since May 2010 is used. It is assumed that the very long wavelength components of the gradients can be reduced by external gravity field information. This assumption has to be made because the gravity data given in a restricted area do not adequately represent the very long wavelength signal. As GOCE is expected to improve the gravity field especially in the medium-wavelength the GOCE data are preliminary reduced by a gravity model up to D/O 49. As a reference model EGM2008 [10] is used throughout these investigations. Although GOCE will be superior to other data types even at higher degree and orders from around D/O 100 to 250, in this case spectral information starting at D/O 50 is used. Hence, using GOCE data at these low degrees may not be an optimal choice, but guarantees that most of the gravity signal that can be detected by GOCE is used in this investigation. In future an optimum combination of GRACE and GOCE data may serve as input data that represents the gravity signal in the best possible way.

First, geoid height solutions are generated from solely GOCE gradient data of the main diagonal tensor components V_{XX}, V_{YY} and V_{ZZ} to investigate the abilities of the two different solution strategies. Following strategy 1, the whole time series of the different gradient types are first filtered in the GRF by applying the Wiener filter method (cf. Eqs. 11-14). The resulting PSDs are exemplarily depicted for the V_{ZZ} gradient in Fig. 5. The noise-free reference signals are simulated from EGM2008, D/O 50 to 250, while the noise PSDs are an adaptation of the ones used in [2]. As Fig. 5 reflects, the resulting spectral content of the filtered signal (magenta curve) is very close to the one of the noise free reference (blue curve) in the measurement bandwidth between 0.005 to.0.1 mHz.

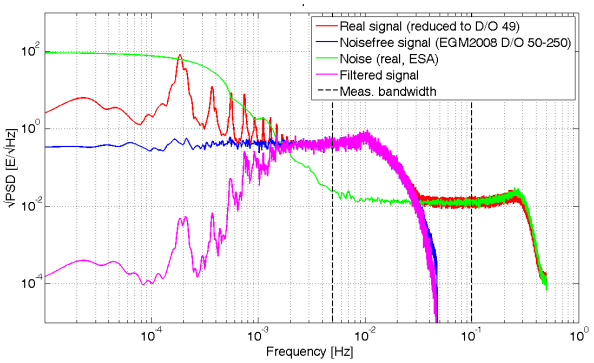

Figure 5. PSD of GOCE V_{ZZ} gradients in GRF from D/O 50 to 250: real GOCE data (red), simulated from EGM2008 (blue), noise from ESA (green) and filtered (magenta)

Applied to the given data configuration, the error covariance function derived from the filter process (Eq. 15) for the filtered V_{ZZ} gradient component is given in Fig. 6 and has a variance of about 500 mE^2 and a correlation length around 200 s.

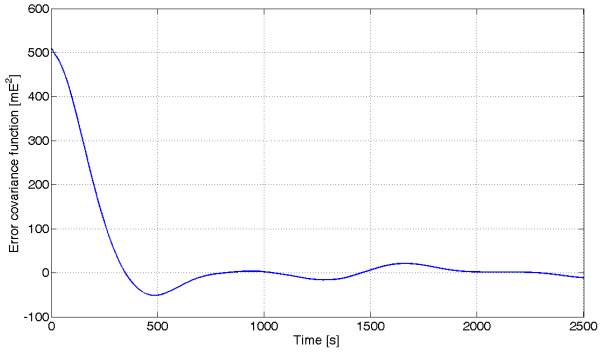

Figure 6. Auto-covariance function of the filter error applying Wiener filtering to GOCE V_{ZZ} gradient time series

To reduce computational efforts, the gradient data is subsequently thinned out to a sampling rate of 5 seconds, and the test area is restricted to 53°-69°E and 73°-78°N, covering the Northern island of Novaya Zemlya, which is displayed in Fig. 7. The resulting data distribution is quite heterogeneous, which is also reflected in the standard deviations of the geoid solutions with LSC (c.f. Fig. 8, right column of panels A and B). Therefore an approach for selecting data in accordance to their relative position might bring a more homogeneous and thus advantageous distribution.

For the derivation of the covariance matrices C_{sl} and C_{ll} of the collocation process (cf. Eq. 1), degree variances of EGM2008 consistent to the spectral information content of the observations from D/O 50 to 250 are used. The noise covariance matrix is set up in GRF using the error covariance functions of the Wiener filtering (cf. Eq. 15 and Fig. 6).

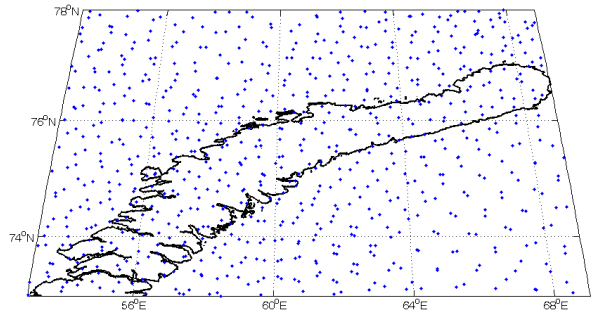

Figure 7. Test area and gradient data distribution for geoid computations

Following the second solution strategy, real V_{XY} and V_{YZ} given in the GRF are replaced by simulated observations from EGM2008 from D/O 50 to 250. Subsequently the gradients are rotated to the LORF where the Wiener filtering is applied. In contrast to strategy 1 the noise covariance matrix C_{nn} has to be rotated from GRF to LORF as well, i.e. it has to be set up in GRF with a-priori stochastic information of the gradient errors. As explained in section 2.3, in case of real data this is obtained from a preceding Wiener filtering in GRF, while for simulated observations, a covariance propagation of EGM2008 is performed.

In Fig. 8 the geoid height results of the two solution strategies are compared within the first two rows. In the left column the differences of the LSC solutions to a reference gravity field derived from EGM2008, D/O 50 to 250, is shown, while the right column represents the spatial distribution of the standard deviation of the LSC results. It can be seen that no obvious differences between strategy 1 and 2 are visible. In both cases, the maximum deviations to the reference amount up to 50 cm or slightly above. The achievable accuracy of the geoid solutions is also very similar with minimum ±12 cm in the central region, highly depending on the data distribution. Close to the test area margins, the

accuracy is decreasing due to edge effects caused by the lack of observations outside the region.

In the next scenario geoid heights are computed by LSC from terrestrial gravity data only. The data for these investigations are simulated in terms of gravity anomalies from EGM2008 on a 0.25°x0.25° grid. This has the advantage to solve for gravity signals of specific spectral resolution, also chosen from D/O 50 to 250, but is still in good agreement with the currently best terrestrial data set of the Arctic Gravity Project (ArcGP). However, this is obvious since ArcGP was integrated into the processing of EGM2008. For the covariance model used in LSC again signal variances from EGM2008 are applied. The standard deviation of the gravity anomalies was assumed to be 3 mGal throughout the whole investigation area. Again the differences to the EGM2008 reference solution and the according standard deviations derived from LSC for this scenario are illustrated in the panel C of Fig. 8. Using solely gravity anomalies, the difference plot in the left column does not show the high-frequent structure as revealed from the gradients-only solution. Instead rather long-wavelength structured differences dominate. Concerning the accuracy of a solution based on gravity anomalies, the standard deviation is down at about ±4 cm in the center, however it increases rapidly towards the region margins. This is a typical effect of regional gravity field solution when using global base functions.

Finally, the two data types, both gradient data and gravity anomalies, are combined in the data configuration explained above. For the treatment of the GOCE gradients, the first solution strategy was chosen. The panel D in Fig. 8 indicates that the combined solution benefits from both, GOCE gradients and ground gravity anomalies. The maximum geoid height differences to the reference are in the range of a few centimetres. The standard deviation of the geoid height

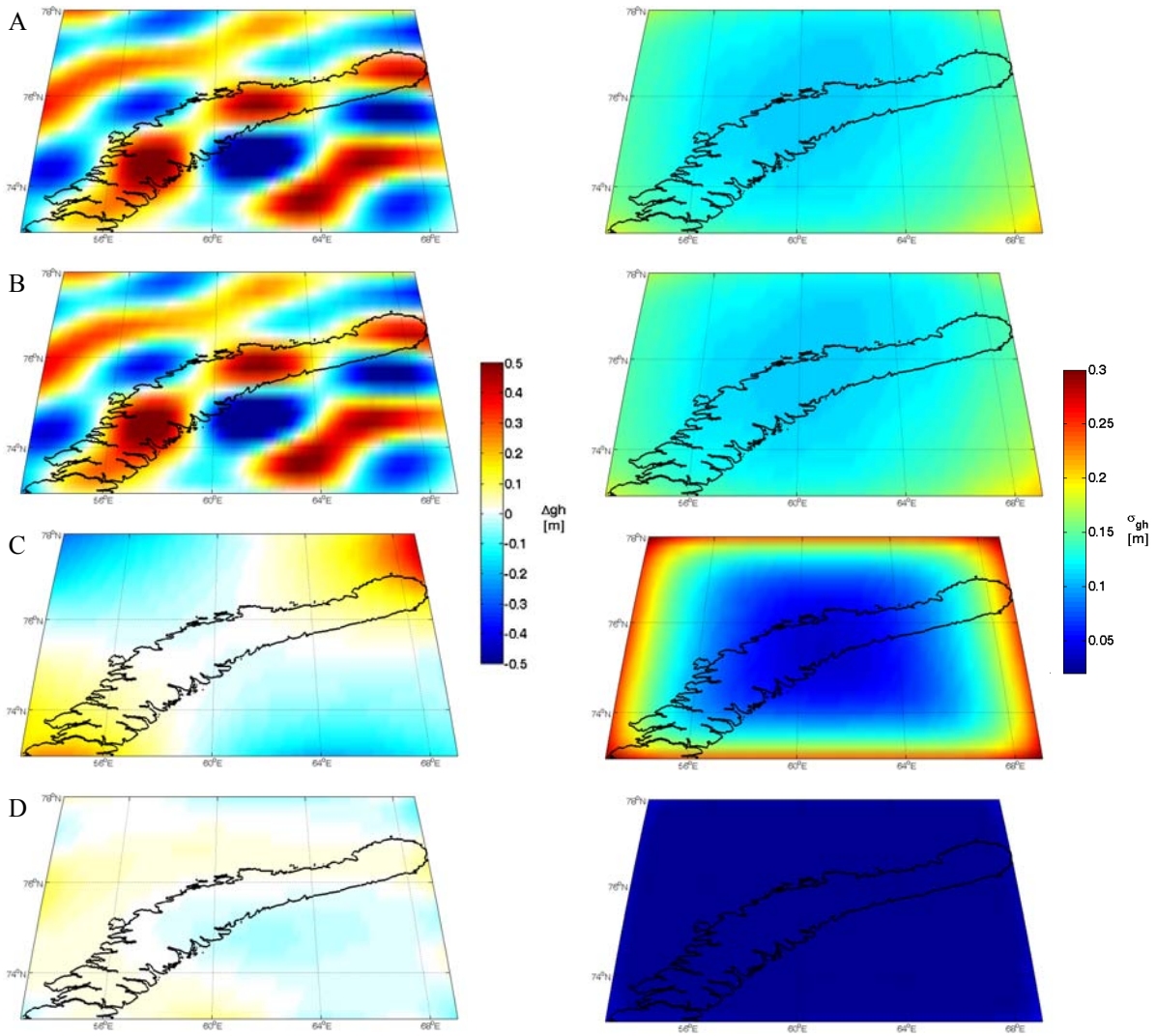

Figure 8. Geoid heights (left) and standard deviations (right) from LSC using GOCE V_{XX}, V_{YY}, V_{ZZ} gradients from November 2009 and reduced to D/O 49 applying strategy 1 (panel A), strategy 2 (panel B), using gravity anomalies from EGM2008 D/O 50 to 250 (panel C) and a combination of both data sources (panel D)

solution is ±2 cm almost homogenously throughout the whole investigated area.

4. DISCUSSION AND CONCLUSIONS

As the results show, using solely GOCE gradients for a LSC geoid solution leads to high deviations to a reference solution derived from EGM2008 up 50 cm and more. At current stage this conclusion is independent of the choice of the solution strategy. The differences may be caused be several problems.

Firstly, both strategies are not free of assumptions that have to be made during the pre-processing of the gradient data. Regarding strategy 1, gradients are Wiener-filtered in the GRF, neglecting the fact that this is not allowed in strict sense in this reference frame. In strategy 2, this is circumvented by a rotation into the LORF, however a-priori information of the less accurate gradient types V_{XY} and V_{YZ} has to be introduced. Furthermore an a-priori knowledge of the stochastic of the observations in the GRF is necessary, which is also based on assumptions.

Additionally, on one hand the gravity field is estimated at ground level, while observations are given at satellite altitude. Thus, the geoid computation can be regarded as downward continuation, which is known to be a unstable procedure. However, the addition of ground data can improve this downward continuation process leading to drastically improvements, as the combination of GOCE and gravity anomalies at ground level has shown.

On the other hand, the choice of a proper covariance function is a problematic issue. When combining both, gradients and gravity anomalies data, the covariance function should reflect the correlations of each data type in the computation area to the best possible extent. The covariance function used in this investigation is based on EGM2008 degree variances. In case of gravity anomalies the model covariance function fits very well to an empirical covariance function of the test area (cf. Fig 9 top). Though, for gradients at orbit altitude the model is slightly overestimating the actual amplitudes of real data (cf. Fig. 9 bottom). Hence a covariance function uniformly valid for each data type has still to be found.

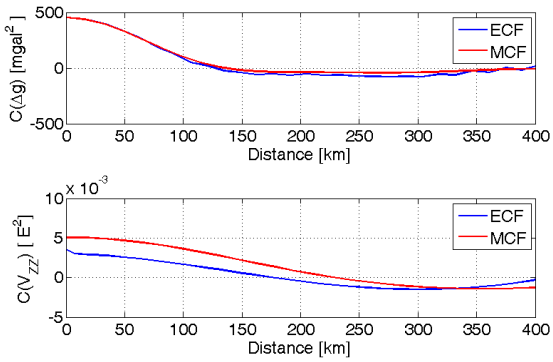

Figure 9. Model (red) and empirical (red) covariance functions based on EGM2008 degree variances for gravity anomalies at ground level (top) and V_{ZZ} gradients at satellite altitude (bottom)

Despite all these open issues, this investigation has shown that the use of GOCE gradients has a tremendous impact on the geoid derivation also at regional scale. Although there are still limitations when estimating the gravity field with gradients only, the combination with ground based gravity data leads to significant improvements of the geoid solutions. This is most obvious in the medium wavelength spectrum of the gravity field signal. However, taking into account the considerations mentioned above, there is still room for further improvements in the future.

5. ACKNOWLEDGEMENTS

This work was performed within the project ICEAGE in the frame of the Austrian Space Applications Programme (ASAP), Phase 5, funded by the Austrian Research Promotion Agency, project number 817106. Special thanks go to all colleagues at our institutions that supported this work with valuable discussions and comments.

6. REFERENCES

1. Albertella A., Migliaccio F., Reguzzoni M & Sansò F. (2004). Wiener filters and collocation in satellite gradiometry. In *International Association of Geodesy Symposia, '5th Hotine-Marussi Symposium on Mathematical Geodesy'*, (Ed. F. Sansò), vol. 127, Springer-Verlag, Berlin, 32-38.

2. Catastini G., Cesare S., De Sanctis S., Dumontel M., Parisch M. & Sechi G. (2006). Predictions of the GOCE in-flight performance with the end-to-end system simulator. In *Proc. 3rd International GOCE User Workshop*, November 2006 Frascati, Italy, ESA SP-627, pp9-16.

3. Migliaccio F., Reguzzoni M. & Sansò F. (2004). Space-wise approach to satellite gravity field

determination in the presence of coloured noise. *Journal of Geodesy*, 78, 304-313.

4. Migliaccio F., Reguzzoni M., Sansò F., Tscherning C.C. & Veicherts M. (2010). GOCE data analysis: the space-wise approach and the first space-wise gravity field model. In *Proceedings of the ESA Living Planet Symposium*, 28 June – 2 July 2010, Bergen, Norway.

5. Moritz H. (1980). *Advanced Physical Geodesy*. Wichmann Verlag, Karlsruhe.

6. Pail, R. (2005). A parametric study on the impact of satellite attitude errors on GOCE gravity field recovery. *Journal of Geodesy*, 79, 231-241.

7. Pail R., Sharov A., Rieser D., Heuberger F., Wack R. & Gisinger C. (2009). Modelling snow-ice cover evolution and associated gravitational effects with GOCE constraints. Poster, EGU General Assembly 2009, Vienna, Austria.

8. Pail R., Goiginger H., Mayrhofer R., Schuh W.-D., Brockmann J.M., Krasbutter I., Höck E. & Fecher T. (2010).GOCE gravity field model derived from orbit and gradiometry data applying the time-wise method. GOCE gravity field model derived from orbit and gradiometry data applying the time-wise method. In *Proceedings of the ESA Living Planet Symposium*, 28 June – 2 July 2010, Bergen, Norway.

9. Papoulis A. (1984). *Signal analysis*. McGraw Hill, New York.

10. Pavlis N., Holmes S., Kenyon S. & Factor J. (2008). EGM2008: An Overview of its Development and Evaluation. Presentation at the IAG International Symposium Gravity, Geoid and Earth Observation 2008, 23-27 June 2008, Chania, Crete, Greece.

11 .Tscherning C.C. & Rapp R.H. (1974). Closed covariance expressions for gravity anomalies, geoid undulations, and deflections of the vertical implied by anomaly degree variance models. *Reports of the Department of Geodetic Science*, Rep. No. 208, Ohio State University, Columbus, Ohio.

12. Tscherning C.C. (1976). Covariance expressions for second and lower order derivatives of the anomalous potential. *Reports of the Department of Geodetic Science*, Rep. No. 225, Ohio State University, Columbus, Ohio.

13. Tscherning C.C. (1993). Computation of covariances of derivatives of the anomalous gravity potential in a rotated reference frame. *Manuscripta Geodetica*, Vol. 18, no. 3, pp 115-123.